Photodissociation Spectra for Size-Selected $Sr^+(CH_3OH)_n$ and $Sr^+(CH_3OD)_n$ Clusters†

James I. Lee,‡ Jun Qian,§ David C. Sperry,# Anthony J. Midey, Jr.,⊥ Stephen G. Donnelly,|| and James M. Farrar*

Department of Chemistry, University of Rochester, Rochester, New York 14627

Received: March 8, 2002; In Final Form: June 27, 2002

This study presents photodissociation data on the mass-selected clusters $Sr^+(CH_3OH)_n$ and $Sr^+(CH_3OD)_n$, $n = 1-4$, in the wavelength range from 310 to 1500 nm. The parent ion clusters exhibit loss of hydrogen atoms by C−H bond cleavage in their ground electronic states, a channel that increases in magnitude with increasing cluster size. Electronic states of clusters based on excitation of metal-centered d, p ← s transitions are observed. The cluster spectra exhibit a size-dependent red shift that is consistent with increased metal−ligand repulsion with increasing size. The clusters decay by solvent evaporation, methyl radical loss to form the metal hydroxide cation, and loss of oxygen-bound hydrogen atoms to form the metal methoxide cation, $SrOCH_3^+$.

Introduction

Spectroscopic studies of stepwise-solvated alkaline earth cation clusters provide detailed microscopic insight into the solvation process by probing the local electronic environment of the metal ion valence electron as a function of cluster size. Metal-centered clusters are especially interesting as models for spontaneous ionization and electron solvation in condensed phases and for ion solvation in bulk solutions. A number of studies of alkaline earth cations have appeared in the literature, some with the objective of providing a high-resolution view of the electrostatic binding in ion−solvent complexes,[1−3] while others have focused on the size dependences of the electronic states in such systems and the reactivities in those states.[4−9] In favorable cases, vibrationally[10−14] and rotationally[15] resolved electronic spectra provide a high-resolution view of the solvation process. Theoretical calculations are invaluable in assigning the observed electronic bands[16,17] and vibrational and rotational frequencies.[18,19] Theoretical calculations also reveal complexities induced by electronic state mixing in systems with low-lying d orbitals. The ligand electric field perturbs the electronic structure of the metal atom and mixes d character into the s and p orbitals, allowing electronic transitions with nominal d ← s character.[16,17]

Several previous studies have shown that chemical reaction can occur in the ground electronic states of clusters comprised of singly charged alkaline earth ions solvated by polar solvents.[5,20−26] Fuke and co-workers have shown a number of examples in their work with $M^+(H_2O)_n$ (M^+ = Ca or Mg),[5,20,21] in which solvated hydroxide $(MOH^+)H_2O$ cluster ions formed by chemical reaction on the ground electronic surface dominate over the solvated metal ions in certain cluster-size regimes. This phenomenon has become known as a "product switching". A similar effect has been observed in alkali metal clusters $M^+(CH_3OH)_n$ (M^+ = Na, Cs) as probed by vibrational predissociation spectroscopy by Selegue and Lisy.[27] The clusters are shown to eliminate dimethyl ether to form $M^+(CH_3OH)_{n-2}(H_2O)$, a reaction channel that gains intensity with increasing cluster size.

Absorption spectroscopy is only one method that can probe the solvation process. Experiments in which more than one decay channel is induced by photon absorption and for which product branching ratios are determined as a function of excitation wavelength are especially useful in assessing reaction pathways and probing key features of excited and ground-state potential energy surfaces. Recent work from the Kleiber group[25,26] demonstrates that point in studies of C−H and C−O bond activation in clusters of Mg^+ bound to acetaldehyde, CH_3-CHO.

Often, thermochemical data provide clear explanations for why one product channel is favored over another. Experiments in high-pressure[23,28,29] and high-temperature[30,31] mass spectrometry in conjunction with theoretical binding energy calculations[32−34] are indispensable in estimating reaction threshold energies. Distinguishing between processes that occur on the ground state or excited electronic state surfaces provides incisive information on the solvation process.

In this paper, we present a study of the ground-state and excited-state reaction channels that occur in clusters of the alkaline earth cation Sr^+ solvated by CH_3OH and CH_3OD. In the parent mass spectra, we observe a ground electronic state reaction in both systems that eliminates at least one H atom by C−H bond cleavage, causing a "product switching" at $n = 4$ in $Sr^+(CH_3OD)_n$. We also report the photodissociation spectroscopy of $Sr^+(CH_3OH)_n$ and $Sr^+(CH_3OD)_n$, and discuss reaction processes that result in evaporation of solvent, C−O bond cleavage to form $SrOD^+$, and formation of $SrOCH_3^+$ by O−D bond rupture. This work complements recent reports on the related Mg^+ system studied by photodissociation in our lab[9] and by collision-induced dissociation in the laboratory of Armentrout and co-workers.[35]

† Part of the special issue "Jack Beauchamp Festschrift".

* To whom correspondence should be addressed.

‡ Present address: Stanford Research Systems, 1282 Reamwood Avenue, Sunnyvale, CA 94089.

§ Present address: Aerospace Corporation, El Segundo, CA 90245.

Present address: Pharmacia-Upjohn, 7000 Portage Road, Kalamazoo, MI 49001.

⊥ Present address: Air Force Research Laboratory, VSBP, Hanscom Field, MA 01731.

|| Present address: National Center for Atmospheric Research, Boulder, CO 80309.

10.1021/jp020666a CCC: $22.00
Published on Web 08/23/2002

Experimental Section

The experimental apparatus for these experiments has been described in detail previously;[36] only the most salient points are mentioned here. Helium at ~1.5 atm is bubbled through CH_3OH (Aldrich spectrophotometric grade, 99.9%) or CH_3OD (Cambridge Isotopes, 99% D) that is heated to produce an ~30% mixture of methanol vapor in He. This seeded vapor is adiabatically expanded through a solenoid-driven pulsed valve (General Valve, series 9) into a laser vaporization ion source. Strontium metal (Aldrich, 99%) is ablated and ionized by focused second harmonic radiation from a Nd^{3+}:YAG laser (Continuum, NY-61). The seeded vapor is forced through the Sr^+ plasma, creating a distribution of cluster sizes, Sr^+-(methanol)$_n$. Typically, the pressure in the cluster source chamber is $\sim 10^{-5}$ Torr. The clusters are collisionally cooled as they travel in a supersonic expansion down a channel into the source chamber. They then enter the extraction region of a Wiley−McLaren-type time-of-flight mass spectrometer. The clusters reach a mass-independent spatial focus 1.5 m downstream from this region. The clusters are photolyzed by radiation that transversely intersects the cluster beam at the spatial focus. This radiation is provided by a narrow bandwidth (~0.2 cm^{-1}) singly resonant optical parametric oscillator (OPO) (Spectra Physics, MOPO-730). The OPO signal wave tuning range is from 440 to 690 nm, and its idler wave tuning range is from 730 to 1830 nm. The OPO is also equipped with a frequency doubling option (FDO) allowing the OPO to produce ultraviolet radiation. The FDO tunes from 220 to 345 nm by doubling signal frequencies and from 366 to 450 nm by doubling idler frequencies. The OPO is pumped by the third harmonic of an injection-seeded Nd^{3+}:YAG laser (Spectra Physics, GCR-190) running at 10 Hz. Photodissociation creates a distribution of product and unphotolyzed reactant ions, which are separated using a reflectron-type mass spectrometer. A set of off-axis microchannel plates detects and amplifies the signal. The data are typically averaged over 100 laser shots (DSP, 4101) and a transient recorder (DSP, 2100AS) sends the data from a CAMAC crate to a PC. Photodissociation laser power was monitored throughout the experiment and kept at a constant value of 1 mJ/pulse.

Results

Mass and Photodissociation Spectroscopy. Parent mass spectra of Sr^+(methanol)$_n$ are shown in Figure 1. The loss of a H atom from $^{88}Sr^+(CH_3OH)_n$ creates a $^{88}Sr^+CH_2OH(CH_3OH)_{n-1}$ product that is isobaric with the $^{87}Sr^+(CH_3OH)_n$ isotopomer of the parent. When C−H bonds are cleaved in two methanol molecules, the resultant product overlaps with the $^{86}Sr^+(CH_3OH)_n$ isotopomer mass peak. The apparent intensities of clusters based on the ^{87}Sr and ^{86}Sr isotopes are therefore larger than predicted on the basis of natural isotopic abundances, an observation easily seen in Figure 1 as the cluster size increases. Examining the $Sr^+(CH_3OD)_n$ parent mass spectra shows the same effect, proving that a hydrogen atom is lost from the C−H rather than the O−H (D) bond. If deuterium atoms were lost exclusively, there should be a 2 amu spacing between those products. One would expect to break the C−H bond rather than the O−H (D) bond given the bond strengths involved; in methanol, the O−H bond requires 10 kcal/mol more energy to cleave than the C−H bond.[37] These results contrast with those reported by Lu and Yang, who have published parent ion mass spectra on the $Sr^+(CH_3OH)_n$ system,[22] reporting essentially the same mass spectra shown here, but ascribing the H loss to cleavage of the O−H rather than the C−H bond. One may argue

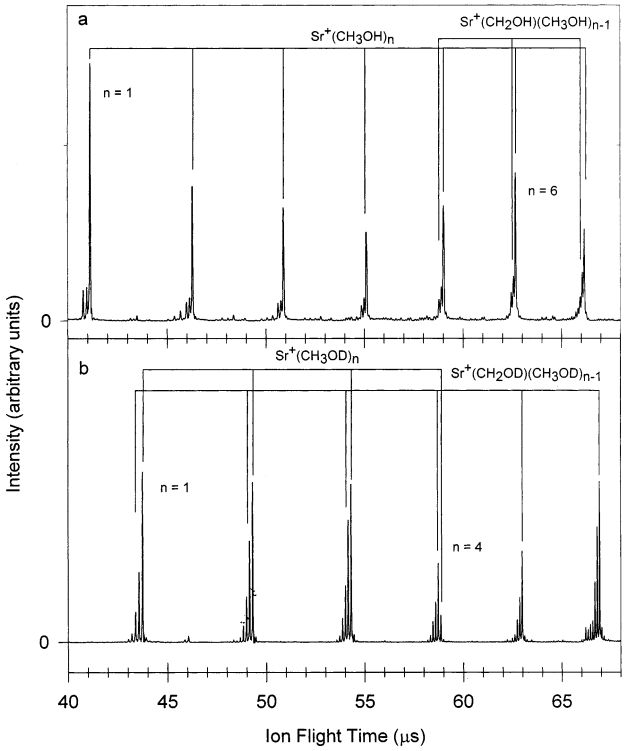

Figure 1. Parent mass spectra of (a) $Sr^+(CH_3OH)_n$ and (b) $Sr^+(CH_3OD)$. Both the deuterated and undeuterated mass spectra are consistent with loss of H from the methyl moiety. This reaction is favored with solvation as is demonstrated by the increase in the H loss peaks, gaining intensity with increasing cluster size.

that a combination of H and D atoms is eliminated to create the mass peaks that we observe on the lighter mass side of the 87 isotopomer peak. Further studies using different isotopomers of methanol are required to prove which bonds are cleaved to create these products, but the consistent 1 amu spacing in both $Sr^+(CH_3OH)_n$ and $Sr^+(CH_3OD)_n$ strongly suggests the C−H bond is broken successively. Hereafter, when referring to a particular cluster, we will always mean one composed of the most abundant $^{88}Sr^+$ isotope.

The clusters are created by a Sr^+(methanol)$_{n+m}$ parent that has been cooled by evaporating m solvent molecules. The larger clusters retain significant internal energy,[38,39] making cleavage of the C−H bond more facile in these clusters. When $n = 4$ in the $Sr^+(CH_3OD)_n$ system, the loss of H has become the dominant ground-state reaction pathway, and the most intense species observed is $^{88}Sr^+(CH_3OD)_3CH_2OD$. This "product switching" phenomenon has been observed independently by Fuke and co-workers[20] in the $Ca^+(H_2O)_n$ system, in which the $(CaOH^+)(H_2O)_n$ species dominates the mass spectrum beginning at $n = 5$, and in our work on the $Sr^+(H_2O/D_2O)_n$ systems,[11] in which we observe product switching to the metal hydroxide around $n = 5-6$.

Preliminary data on the photodissociation spectra of $Sr^+(CH_3OH)$[10] in the visible region and of $Sr^+(CH_3OH)_{2-4}$[36] in the region from 550 to 920 nm have been published previously. The addition of frequency doubling capabilities to our OPO system allows us to probe electronic transitions that occur in the ultraviolet region. Figure 2 shows the complete spectra acquired for $Sr^+(CH_3OH)_n$ and $Sr^+(CH_3OD)_n$ with $n = 1-4$. To the best of our knowledge, calculations on the vertical transition energies of Sr^+(methanol)$_n$ do not yet exist. Therefore, we have used ab initio calculations on the $Sr^+(H_2O)_n$ system by Bauschlicher et al.[16] as a guide for assignment of the

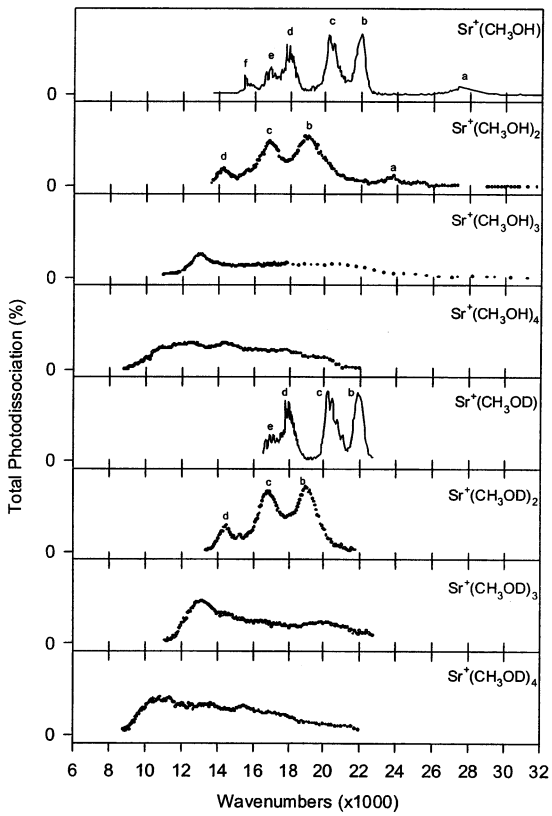

Figure 2. Photodissociation spectra of $Sr^+(CH_3OH)_n$ and $Sr^+(CH_3OD)_n$. $Sr^+(CH_3OD)_n$ was not interrogated with UV wavelengths. Monomer and dimer spectral maxima are labeled with letters a−f, which are assigned to transitions from the ground electronic state to the following states: (a) $(6)^2A'$ (5pσ); (b) $(3)^2A''$ (o-p 5pπ); (c) $(5)^2A'$ (i-p 5pπ); (d) $(4)^2A'$ (4dσ); (e) $(2)^2A''$ (o-p 4dπ); (f) $(3)^2A'$ (i-p 4dπ). Table 1 compares these assignments to ab initio calculations on $Sr^+(H_2O)$ (ref 16).

electronic transitions. Table 1 summarizes the positions of calculated and observed electronic transitions, labels their symmetries, and indicates whether the excited orbitals involved are in the plane (i-p) of the metal−ligand bond or out of this plane (o-p) for $Sr^+(CH_3OH)_{1,2}$. The details of these band assignments are left to the discussion and will be only generally described here.

In $Sr^+(CH_3OH)$, which we refer to as the "monomer", there are six resolved bands, ranging in energy from approximately 15 000 to 27 000 cm^{-1}. In analogy with ab initio calculations on the $Sr^+(H_2O)$ system,[16] we assign the highest energy band in $Sr^+(CH_3OH)$ as a transition to a 5pσ-like state. The observation of this band completes the assignment of transitions based on excitation of 5p-based molecular orbitals.[10] Below the 5pσ band, we find two well-resolved electronic bands, which we attribute to transitions to 5pπ-like states. The bands that appear in the low-energy portion of the monomer spectrum correspond to transitions to states with 4d atomic character. The partially resolved vibrational structure in the 4dσ and 4dπ bands has been discussed previously.[10,40]

In the dimer, $Sr^+(CH_3OH)_2$, we find spectral features that we treat as originating from a broadened and red-shifted monomer spectrum. We tentatively assign a 5pσ-like band near 23 500 cm^{-1} and two 5pπ-like bands near 17 000 and 19 000 cm^{-1}. The spectral breadths of the triply and quadruply solvated species, that is, the trimer and the tetramer, preclude any definitive band assignment in these clusters.

Photochemical Channels. Identification of the dissociation channels in the monomer, $Sr^+(CH_3OD)$, provides a baseline for interpreting the decay channels in the larger clusters. The dissociation channels that can occur by single-photon absorption are listed here:

$$Sr^+(CH_3OD) \rightarrow Sr^+ + CH_3OD \quad (-L)$$
$$\rightarrow SrOD^+ + CH_3 \quad (-Me)$$
$$\rightarrow SrOCH_3^+ + D \quad (-D)$$

The notation for the decay channels (−L, −Me, −D) is that introduced in our work on the related $Mg^+(CH_3OD)_n$ systems.[9] Solvent evaporation is denoted as −L, methyl loss via C−O bond cleavage as −Me, and deuterium atom loss by O−D bond cleavage as −D. The first two of these channels were reported in our earlier paper on $Sr^+(CH_3OD)$ dissociation,[10] but the loss of hydrogen atoms from oxygen was not reported. The proper observation of this last channel requires isotopic labeling and very careful mass spectrometry. Because of the importance of evaluating the D-loss channel quantitatively in the interpretation of the dissociation dynamics, we restrict our discussion to clusters based on CH_3OD.

Figure 3 shows photodissociation mass spectra of the unreacted "parent" ions $Sr^+(CH_3OD)_n$, $n = 1-4$, and all photochemical products or "daughter" ions that were detected at selected photolysis wavelengths. In the monomer ($n = 1$), signals from all three channels are observed. In the dimer ($n = 2$), all three channels are observed, but in addition, the data show these three channels in concert with ligand loss, denoted as −(L + D), −(L + Me), and −2L. In the trimer, ($n = 3$), with photolysis occurring at 594 nm, we observe the baseline channels corresponding to −L, −D, and −Me. In addition, we see those same channels accompanied by loss of one or more

TABLE 1: Comparison of Experimental $Sr^+(CH_3OH)_{1,2}$ and Calculated $Sr^+(H_2O)_{1,2}$ Spectral Maxima

exptl $Sr^+(CH_3OH)$		calcd $Sr^+(H_2O)$[16]		exptl $Sr^+(CH_3OH)_2$		calcd $Sr^+(H_2O)_2$[16]	
state[a]	energy (cm^{-1})	state	energy (cm^{-1})	state	energy (cm^{-1})	state	energy (cm^{-1})[b]
$(1)^2A''$ (4dδ)	unobsd	$(2)^2A_1$ (4dδ)	14 700				
$(2)^2A'$ (4dδ)	unobsd	$(1)^2A_2$ (4dδ)	14 800				
$(3)^2A'$ (i-p 4dπ) (f)	∼15 800	$(1)^2B_2$ (4dπ)	16 000			$(2)^2E$ (4dπ)	20 400 (S)
$(2)^2A''$ (o-p 4dπ) (e)	∼16 400	$(1)^2B_1$ (4dπ)	17 000				
$(4)^2A'$ (4dσ) (d)	∼17 500	$(3)^2A_1$ (4dσ)	18 038	$(4)^2A'$ (4dσ) (d)	∼14 300		
$(5)^2A'$ (i-p 5pπ) (c)	∼20 200	$(2)^2B_2$ (5pπ)	21 400	$(5)^2A'$ (i-p 5pπ) (c)	∼16 600	$(1)^2B_{3u}$ (5pπ)	18 800 (E)
						$(1)^2E$ (5pπ)	18 800 (S)
$(3)^2A''$ (o-p 5pπ) (b)	∼22 000	$(2)^2B_1$ (5pπ)	22 900	$(3)^2A''$ (o-p 5pπ) (b)	∼19 000	$(1)^2B_{2u}$ (5pπ)	20 900 (E)
$(6)^2A'$ (5pσ)[c] (a)	∼27 000	$(4)^2A_1$ (5pσ)	<26 000	$(6)^2A'$ (5pσ)[c] (a)	∼23 500	$(1)^2B_{1u}$ (5pσ)	23 300 (E)
						$(2)^2B_2$ (5pσ)	23 700 (S)

[a] Electronic state designations a−f are also shown in Figure 2. [b] (E) refers to a calculation on the eclipsed conformation of $Sr^+(H_2O)_2$, (S) to the staggered conformation. [c] The state labeled $(3)^2A'$ in our previous publication (ref 10) should read $(6)^2A'$.

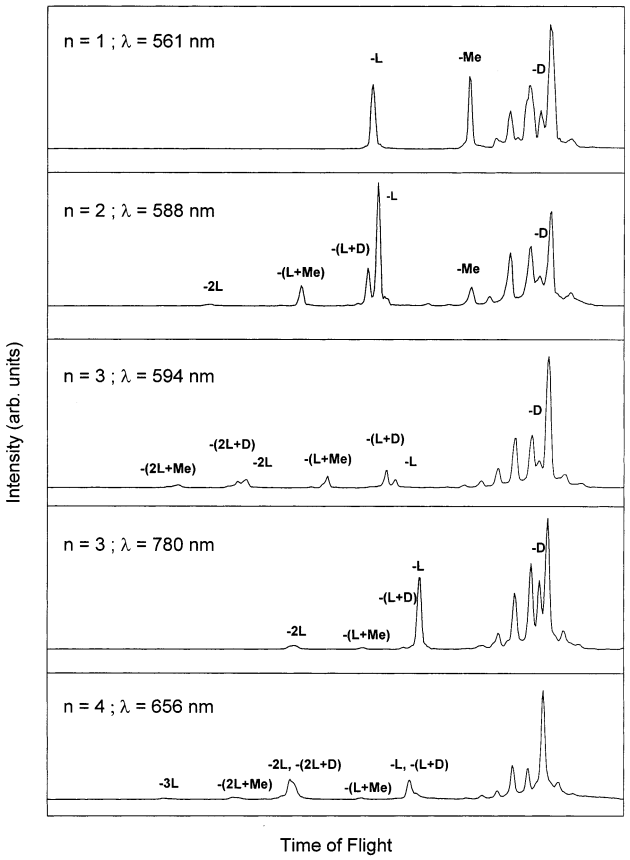

Figure 3. Dissociation of a mass-selected "parent" ion peak to create "daughter" mass spectra at a single photolysis wavelength. We use the following shorthand notation to refer to the photolysis product peaks: −D = loss of deuterium atom; −Me = loss of a methyl fragment; −L = loss of an entire ligand. Combinations of these loss channels are denoted by the symbols listed combined with a + sign. In the case of multiple ligand loss, a coefficient equal to the number of ligands lost precedes the L symbol.

solvent molecules at shorter flight times. When the mass spectrum for the trimer is taken with a longer photolysis wavelength of 780 nm, much less extensive photofragmentation is observed. With the decrease in larger fragments comes an increase in the signal arising from loss of a single ligand. In the tetramer ($n = 4$), the amounts of single ligand loss (−L) and D-loss are substantially reduced relative to the smaller clusters.

A detailed analysis of the fragmentation data suggests that the clusters may absorb more than one photon before decaying. The primary single-photon decay channels are the −L, −D, and −Me pathways. In a separate publication,[41] we analyze fragmentation data for this sequential photon absorption mechanism. In the present paper, we focus attention on the primary channels arising from single-photon absorption in the monomer. Branching ratio data for these channels in the monomer are shown in Figure 4 and illustrate that at low photolysis energies the −D channel is the dominant species, accounting for 80% of the fragments. With increasing photolysis energy, the −Me channel becomes increasingly important and dominates the spectrum in the bands belonging to 5p-based excitations. This result is consistent with our earlier report.[10] The data also confirm the interesting anticorrelation of reactive channels with absorption resonances in the 4d-based electronic states, suggestive of a bond insertion mechanism. A full discussion of the fragmentation channels in clusters larger than the monomer requires explicit consideration of sequential photon absorption.[41]

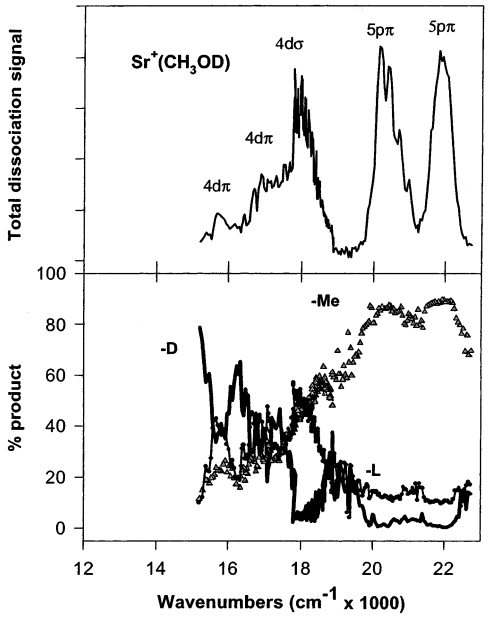

Figure 4. Photodissociation spectrum (top panel) for $Sr^+(CH_3OD)$ and (bottom panel) branching fractions for ligand loss (−L), methyl loss (−Me), and deuterium atom loss (−D).

Discussion

Photodissociation Spectroscopy. The electronic transitions of the singly solvated cluster, the monomer, in the visible region have already been published in our previous letter.[10] In this publication, we report observation of a band in the ultraviolet at 27 000 cm^{-1}. Bauschlicher's calculations predict that a $(4)^2A_1 \leftarrow (1)^2A_1$ transition will occur in $Sr^+(H_2O)$ at 26 000 cm^{-1}, and the onset of the ultraviolet band that we observe occurs near 25 000 cm^{-1}.[11] This transition in the C_{2v} symmetry point group of $Sr^+(H_2O)$ corresponds to a $(6)^2A' \leftarrow (1)^2A'$ transition in the C_s symmetry of $Sr^+(CH_3OH)$, and because the energetics of the transitions also correspond, we are confident in assigning the $(6)^2A' \leftarrow (1)^2A'$ transition to the observed band at about 27 000 cm^{-1}.

Calculations on $Sr^+(H_2O)_2$[16] have shown that the ligand configurations corresponding to eclipsed and staggered conformers are minima on the potential energy surface. The eclipsed arrangement holds the ligands in the same plane as the O−Sr−O bond, while in the staggered conformer the ligands are mutually perpendicular. The calculations also show that the potential energy barrier to interconversion is low and flat. If the clusters are sufficiently warm, the spectra may represent a conformational averages. It is very likely that the sdσ hybridization leading to a linear O−Sr−O geometry[16] will also occur in $Sr^+(CH_3OH)_2$. Given this geometry, one would expect the barriers to rotation for $Sr^+(CH_3OH)_2$ and $Sr^+(H_2O)_2$ to be similar, with barrier for the former system slightly larger in magnitude. We therefore assume that our dimer photodissociation spectrum is probably an average of the eclipsed and staggered conformers.

The dimer photodissociation spectrum of Figure 2 displays four distinct electronic bands, labeled a through d and listed in Table 1. Those transitions appear to be related to the corresponding four transitions in the monomer, for which Bauschlicher has reported assignments, also summarized in Table 1.[16] The lowest-energy transition in the dimer is similar in appearance to the monomer band assigned to excitation of a state with significant 4dσ character. Based on the correspondence between monomer and dimer transitions, this assignment is more

plausible than one based on distinctions between staggered and eclipsed conformations in the dimer, which in $Sr^+(H_2O)_2$ are separated by at most 500 cm^{-1}.

The dissociation spectra summed over all product channels for all cluster sizes are plotted in Figure 2. The most obvious general trend in the spectra is the broadening and red shifts that occur with increasing cluster size. The broadening occurs in large part because of inefficient cooling of the larger clusters. These clusters are probably created by larger precursors that have undergone solvent evaporation. Clusters created this way retain significant internal energy, as previously discussed. The density of accessible states increases with increasing cluster size, so spectral congestion also contributes to the broadening. The existence of conformational isomers may also cause inhomogeneous broadening in the spectra. The spectral red shifts were also observed in the $Sr^+(H_2O)_n$ system[11,42] and verified by theoretical calculations by Bauschlicher, Sodupe, and Partridge.[16] The calculations reveal that increased metal−ligand repulsion occurs with increasing cluster size and raises the 5s orbital in energy, decreasing the energy difference between the ground and excited electronic states. Similar interactions are likely responsible for the same red shifts that we observe in the $Sr^+(methanol)_n$ system.

As Sperry et al. suggest in their discussion on the $Sr^+(H_2O/D_2O)_n$ systems,[11] the sharp rise at the longest wavelengths may occur as a result of a change in electronic state ordering. The same arguments are likely to be valid in the corresponding methanol-based clusters. $Sr^+(H_2O)_3$ is "T"-shaped,[16] which places two of the p orbitals in the plane of the heavy atoms in an σ-type interaction, while the third p orbital is perpendicular to this plane. The d orbitals are each involved in σ-like interactions as well.[11] The σ-type interaction is destabilized though metal−ligand repulsion and raises valence states significantly in energy. This phenomenon is demonstrated by the relative energy separation between the pπ- and pσ-like states in $Sr^+(water)_n$ and $Sr^+(methanol)_n$. In both systems, the pσ state is accessed at energies thousands of wavenumbers higher than the pπ-states.

Thus, in accordance with calculations on the level ordering by Bauschlicher et al.,[16] we suggest that a pπ-type interaction occurs for clusters of size $n > 2$ in $Sr^+(water)_n$, which is responsible for the rapid intensity increase in the red end of the spectra. Given the similarity of state ordering between the monomers of both systems and the similarity of the spectra for the clusters sized $n > 2$, we suggest the pπ-type interaction discussed in the $Sr^+(water)_n$ systems also occurs in $Sr^+(methanol)_n$.

Photochemical Product Channels. Solvation energies of Sr^+ by methanol are not reported in the literature, to the best of our knowledge. Comparison with the literature values for the $Sr^+(H_2O)_n$ system allows us to obtain reasonable estimates of the binding energies. On the basis of the dipole moments and polarizibilities of the water and methanol, we expect the ligand binding energies to be similar in both systems, perhaps slightly weaker in $Sr^+(CH_3OD)_n$. The ligand binding energies of $Sr^+(H_2O)_n$ reported by Bauschlicher et al. represent reasonable upper limits for the corresponding bond energies in $Sr^+(CH_3OD)_n$. The calculated energies are approximately 7 kcal/mol smaller than high-pressure mass spectrometry results reported by Tang et al.[28] for the ligand binding energy of $Sr^+(H_2O)$. Our recent paper[11] on $Sr^+(H_2O)_n/Sr^+(D_2O)_n$ suggests that the experimental value of Tang et al.[28] is too high. As a result, we have decreased our estimate of the monomer ligand loss channel endothermicity by 7 kcal/mol to reflect the 23 kcal/mol value for the monomer ligand binding energy of $Sr^+(H_2O)$ found by Bauschlicher and co-workers.[16]

We use a simple thermodynamic cycle to estimate the endothermicities of the bond cleavage channels, corresponding to −D and −Me. Summing the enthalpies of the ligand binding energy, the C−O bond strength in methanol,[37] and the Sr−O bond strength in $SrOH^+$ [31] yields an estimate of 10 kcal/mol for the methyl loss channel. The cycle is of less use in the case of −D, because a value for the Sr^+-OCH_3 bond strength is unknown. We can obtain the minimum endoergicity for this channel by simply substituting the Sr^+-OH bond enthalpy measured by Murad[31] for the Sr^+-OCH_3 bond enthalpy; this places the −D channel at least 22 kcal/mol above $Sr^+(CH_3OD)$. Both the −Me and −D reaction pathways involve bond formation as well as bond scission. Therefore, we expect both of these channels to proceed over activation energy barriers.

In the $Sr^+(CH_3OD)$ experimental data, we find trends that provide insight into the potential energy barriers for the −Me and −D channels. At the longest photolysis wavelengths, the −D channel is in strong competition with the −L channel, consistent with the comparable endoergicities for each channel. However, the least endoergic channel, −Me, is nearly absent at the very red end of the spectrum. Furthermore, −Me does not become a dominant channel until the much higher energy 5pπ bands are accessed. The data suggest that the barrier for methyl loss is higher than that for D loss.

Crossed molecular beam work by Davis et al.[43] on the related Ba + CH_3OH system provides insight into this issue. In their experiments, Davis and co-workers found that both ground (^1S) and excited (^1D) electronic state Ba produced the $BaOCH_3$ (−H) product almost exclusively, although the BaOH (−Me) channel is less endoergic. This remarkable selectivity is explained in terms of expected relative potential energy barriers. The most likely pathway for elimination of H is through a migration mechanism. The spherical symmetry of the 1s orbital of H allows simultaneous overlap with both the metal and the oxygen atom on CH_3OH, thereby facilitating a migration. In contrast, the elimination of a methyl radical is expected to proceed only when the $O-CH_3$ bond is nearly broken, suggesting a substantial potential energy barrier to this reaction. These conclusions are supported by ab initio calculations on transition metal catalyst activation of H−H and $H-CH_3$ bonds, which found the H−H bond was facile to activate, whereas insertion to allow an $H-M-CH_3$ intermediate encountered a substantial potential energy barrier.[44,45] The work of Sulzbach et al.[46] on hydrogen atom and methyl radical migration in dialkyl carbenes also supports the claim the methyl barrier is considerably higher than that for H migration.

The notion that the barrier for the −D channel is lower than that for the −Me channel is consistent with our experimental observations. All channels are energetically accessible throughout the photon energy range of these experiments, but at lower photon energies, the less restricted transition states for the −D and −L channels dominate the dissociation kinetics. The data support the idea that the −D channel proceeds through a migration process over a lower barrier than that of the insertion process leading to methyl loss. Therefore, at low photolysis energies, the −D channel and the solvent evaporation channel, which we expect to occur without a barrier in excess of the endoergicity, dominate over −Me. However, well above the threshold for the −Me channel, the constraints of the higher barrier are much less restrictive, and that product becomes strongly favored, as is shown in the branching ratio data for the 5pπ bands.

We also note the −D loss channel is only accessed in the lowest energy portion of the spectrum and that it competes very effectively with the ligand loss channel in this wavelength regime. We expect the simple evaporation of ligand to occur directly, without overcoming a potential energy barrier, and therefore, one might expect the −D channel to be a minor process in this portion of the spectrum. The −D channel remains of intensity comparable to ligand loss. The transitions to low-lying d orbitals of Sr^+ are excited in this region of the spectra. As Sanekata et al. proposed in their work on the $Ca^+(H_2O)_n$ system, the proximity of the ^{2}D-derived states to the ground electronic state may facilitate IC and allow more facile elimination of a deuterium atom relative to the higher-lying states of ^{2}P character.[20] We believe this issue may be an important factor in $Sr^+(CH_3OD)_n$ as well and leads to the effective competition of the −D channel with −L throughout the electronic bands based on Sr^+ 4d orbitals in the low photolysis energy regions of the spectra. This situation contrasts with the $Mg^+(CH_3OD)$ system,[9] in which −Me is the exclusive product over the entire wavelength range, indicative of facile selective overlap of the metal p-orbital with the C−O σ^* antibonding orbital. Thus, the differences in reactivity between the Mg^+ and Sr^+ species are direct manifestations of differences in electronic structure of the metal ions.

Conclusions

We have examined $Sr^+(CH_3OH)_n$ and $Sr^+(CH_3OD)_n$ via mass and photodissociation spectroscopy. The parent mass spectra show a ground-state intracluster reaction channel occurs that cleaves the C−H bond in both isotopomers. This observation is most clearly shown in the $Sr^+(CH_3OD)_n$ system, which displays a product switching to $Sr^+(CH_3OD)_3CH_2OD$ at $n = 4$. The electronic states for the monomer and dimer are assigned using calculations on the $Sr^+(H_2O)_n$ system[16] as a guide. We conclude that the deuterium elimination occurs through a H (D) migration mechanism while methyl loss must proceed via a metal atom insertion followed by isomerization over a potential energy barrier. Theoretical calculations on this system will be very important to verifiy and extend the predictions of this work.

Acknowledgment. We gratefully acknowledge support of this work under National Science Foundation Grant CHE-095-23401. Acknowledgment is also made to the donors of the Petroleum Research Fund, administered by the American Chemical Society, for the partial support of this research. A.J.M. acknowledges support from the University of Rochester as a Sherman Clarke Fellow.

References and Notes

(1) Scurlock, C. T.; Pullins, S. H.; Reddic, J. E.; Duncan, M. A. *J. Chem. Phys.* **1996**, *104*, 4591−4599.
(2) Yeh, C. S.; Pilgrim, J. S.; Willey, K. F.; Robbins, D. L.; Duncan, M. A. *Int. Rev. Phys. Chem.* **1994**, *13*, 231−262.
(3) Duncan, M. A. *Annu. Rev. Phys. Chem.* **1997**, *48*, 69−93.
(4) Kleiber, P. D.; Chen, J. *Int. Rev. Phys. Chem.* **1998**, *17*, 1−34.
(5) Misaizu, F.; Sanekata, M.; Tsukamoto, K.; Fuke, K. *J. Phys. Chem.* **1992**, *96*, 8259−8264.
(6) Misaizu, F.; Sanekata, M.; Fuke, K. *J. Chem. Phys.* **1994**, *100*, 1161−1170.
(7) Shen, M. H.; Farrar, J. M. *J. Chem. Phys.* **1991**, *94*, 3322−3331.
(8) Donnelly, S. G.; Farrar, J. M. *J. Chem. Phys.* **1993**, *98*, 5450−5459.
(9) Lee, J. I.; Sperry, D. C.; Farrar, J. M. *J. Chem. Phys.* **2001**, *114*, 6180−6189.
(10) Qian, J.; Midey, A. J.; Donnelly, S. G.; Lee, J. I.; Farrar, J. M. *Chem. Phys. Lett.* **1995**, *244*, 414−420.
(11) Sperry, D. C.; Midey, A. J.; Lee, J. I.; Qian, J.; Farrar, J. M. *J. Chem. Phys.* **1999**, *111*, 8469−8480.
(12) Ding, L. N.; Yong, M. A.; Kleiber, P. D.; Stwalley, W. C.; Lyrra, A. M. *J. Phys. Chem.* **1993**, *97*, 2181−2185.
(13) Yeh, C. S.; Willey, K. F.; Robbins, D. L.; Duncan, M. A. *Int. J. Mass Spectrom. Ion Processes* **1994**, *131*, 307−317.
(14) Yeh, C. S.; Willey, K. F.; Robbins, D. L.; Pilgrim, J. S.; Duncan, M. A. *Chem. Phys. Lett.* **1992**, *196*, 233−238.
(15) Willey, K. F.; Yeh, C. S.; Robbins, D. L.; Pilgrim, J. S.; Duncan, M. A. *J. Chem. Phys.* **1992**, *97*, 8886−8895.
(16) Bauschlicher, C. W., Jr.; Sodupe, M.; Partridge, H. *J. Chem. Phys.* **1992**, *96*, 4453−4463.
(17) Sodupe, M.; Bauschlicher, C. W., Jr.; Partridge, H. *Chem. Phys. Lett.* **1992**, *192*, 185−194.
(18) Sodupe, M.; Bauschlicher, C. W., Jr. *Chem. Phys. Lett.* **1993**, *212*, 624−630.
(19) Sodupe, M.; Bauschlicher, C. W., Jr. *Chem. Phys. Lett.* **1992**, *195*, 494−499.
(20) Sanekata, M.; Misaizu, F.; Fuke, K. *J. Chem. Phys.* **1996**, *104*, 9768−9778.
(21) Sanekata, M.; Misaizu, F.; Fuke, K.; Iwata, S.; Hashimoto, K. *J. Am. Chem. Soc.* **1995**, *117*, 747−754.
(22) Lu, W.; Yang, S. *J. Phys. Chem. A* **1998**, *102*, 825−840.
(23) Harms, A. C.; Khanna, S. N.; Chen, B.; Castleman, A. W., Jr. *J. Chem. Phys.* **1994**, *100*, 3540−3544.
(24) Sperry, D. C.; Lee, J. I.; Farrar, J. M. *Chem. Phys. Lett.* **1999**, *304*, 350−356.
(25) Lu, W. Y.; Kleiber, P. D. *J. Chem. Phys.* **2001**, *114*, 10288−10293.
(26) Lu, W. Y.; Kleiber, P. D. *Chem. Phys. Lett.* **2001**, *338*, 291−296.
(27) Selegue, T. J.; Lisy, J. M. *J. Am. Chem. Soc.* **1994**, *116*, 4874−4880.
(28) Tang, I. N.; Lian, M. S.; Castleman, A. W., Jr. *J. Chem. Phys.* **1976**, *65*, 4022−4027.
(29) Kochanski, E.; Constantin, E. *J. Chem. Phys.* **1987**, *87*, 1661−1665.
(30) Murad, E. *J. Chem. Phys.* **1983**, *78*, 6611−6613.
(31) Murad, E. *J. Chem. Phys.* **1981**, *75*, 4080−4085.
(32) Bauschlicher, C. W., Jr.; Langhoff, S. R.; Partridge, H.; Rice, J. E.; Komornicki, A. *J. Chem. Phys.* **1991**, *95*, 5142−5148.
(33) Bauschlicher, C. W., Jr.; Partridge, H. *J. Phys. Chem.* **1991**, *95*, 3946−3950.
(34) Sodupe, M.; Bauschlicher, C. W., Jr.; Partridge, H. *J. Chem. Phys.* **1991**, *95*, 9422−9423.
(35) Andersen, A.; Muntean, F.; Walter, D.; Rue, C.; Armentrout, P. B. *J. Phys. Chem. A* **2000**, *104*, 692−705.
(36) Donnelly, S. G.; Schmuttenmaer, C. A.; Qian, J.; Farrar, J. M. *J. Chem. Soc., Faraday Trans.* **1993**, *89*, 1457−1465.
(37) *CRC Handbook of Chemistry and Physics*, 77th ed.; Lide, D. R., Ed.; CRC Press: Boca Raton, Florida, 1997.
(38) Cabarcos, O. M.; Weinheimer, C. J.; Lisy, J. M. *J. Phys. Chem. A* **1999**, *103*, 8777−8791.
(39) Cabarcos, O. M.; Lisy, J. M. *Int. J. Mass Spectrom.* **1999**, *187*, 883−903.
(40) Qian, J. Photodissociation Studies of Size-Selected Solvated Strontium Cation Clusters. Doctoral Dissertation, University of Rochester, Rochester, NY, 1995.
(41) Lee, J. I.; Farrar, J. M., manuscript in preparation.
(42) Shen, M.; Winniczek, J. W.; Farrar, J. M. *J. Phys. Chem.* **1987**, *91*, 6447−6449.
(43) Davis, H. F.; Suits, A. G.; Lee, Y. T.; Alcaraz, C.; Mestdagh, J.-M. *J. Chem. Phys.* **1993**, *98*, 9595−9609.
(44) Low, J. J.; Goddard, W. A. *J. Am. Chem. Soc.* **1986**, *108*, 6115−6128.
(45) Low, J. J.; Goddard, W. A. *J. Am. Chem. Soc.* **1984**, *106*, 8321−8322.
(46) Sulzbach, H. M.; Platz, M. S.; Schaefer, H. F., III; Hadad, C. M. *J. Am. Chem. Soc.* **1997**, *119*, 5682−5689.